Conjugate View Gamma Camera Method for Estimating Tumor Uptake of Iodine-131 Metaiodobenzylguanidine

Barry L. Shulkin, James C. Sisson, Kenneth F. Koral, Brahm Shapiro, Xiaohan Wang, and Jon Johnson

Division of Nuclear Medicine, Department of Internal Medicine, University of Michigan Medical Center, Ann Arbor, Michigan

Therapy with [^{131}I]MIBG has produced partial remissions of malignant pheochromocytomas but not all patients respond. Responses correlate with the quantity of radiation delivered. We developed the conjugate-view method of imaging using ^{131}I reference sources of known radioactivity placed on the surface of the patient and standard nuclear medicine equipment (gamma camera and computer), to estimate tumor uptake of [^{131}I]MIBG. Such an estimate is a first step toward calculating radiation absorbed dose. Three different methods of background subtraction were evaluated with an anthropomorphic phantom and in five patients. In phantom results, measured tumor activity decreased exponentially with a half-life in agreement with that of ^{131}I to within 3%. However, in the phantom studies, in which non-tumor activity is zero, no single method of background subtraction is superior. In patients, two background subtraction methods, which take their estimate from regions immediately surrounding or adjacent to the tumor and reference source, are less sensitive to reference source position and appear more accurate than a third method which uses a background region of interest displaced from the tumor. The agreement of the calculated activity concentration (nCi/g) with that measured by counting portions of the excised tumors gives validation to the method.

J Nucl Med 29:542–548, 1988

In evaluating patients with adrenergic tumors for therapy with iodine-131 metaiodobenzylguanidine ([^{131}I]MIBG), we have developed the conjugate-view method for estimating the uptake of [^{131}I]MIBG by the tumors, which can then be used to determine the absorbed radiation dose. The conjugate-view method employs the geometric mean of counts from conjugate views (180°; anterior and posterior) as originally introduced by Sorenson (*1,2*) and as employed by Thomas et al. (*3–5*) to determine tumor activities. According to Thomas, in their conjugate-view approach, a single, separate transmission measurement is obtained by placing an uncollimated source of radioactivity directly over the tumor location. Our technique uses a calibrated source placed on the skin nearby but not over the tumor on each day of imaging. This source serves as a "reference" tumor to allow comparison of a known amount of radioactivity with that found in the tumor. Since our tumors are small, no correction depending on tumor size is made (that is, in the notation of Thomas, $f = 1$).

The method is designed to reduce errors introduced by soft-tissue attenuation, collimator septal penetration, Compton scatter, and day-to-day variability in instrument sensitivity, all in a single procedure. It uses only standard nuclear medicine equipment (gamma camera and computer) and could serve as a model to estimate uptake and thereby dosimetry of other radiopharmaceuticals. We describe, in this report, our results for tumor uptake of [^{131}I]MIBG and the effects of three specific methods of background subtraction in an anthropomorphic phantom and in five patients. In two of these patients, pheochromocytomas were surgically excised and the calculated results for each method are correlated with values determined by counting samples of the tumor.

Received Mar. 9, 1987; revision accepted Sept. 10, 1987.

For reprints contact: Barry L. Shulkin, MD, University of Michigan Medical Center, Dept. of Internal Medicine, Division of Nuclear Medicine, B1G412 Box 0028, Ann Arbor, MI 48109-0028.

METHODS

A humanoid phantom, (Humanoid Systems, Carson, CA), of soft-tissue equivalent molded sections was used to investigate methods of background subtraction and reference source (RC) placement. The liver, right kidney, pancreas, spleen, and stomach were waterfilled. The shells of these organs were formed of 1/8-in.-thick cellulose acetate butyrate. Figure 1 shows a computed tomographic image of the phantom in the transverse plane at the level of the kidneys. A 4-cm hollow sphere was filled with 4.9 μCi of ^{131}I and placed in the cavity normally occupied by the left kidney, to simulate a kidney tumor. Child's modeling clay, with an attenuation coefficient 0.166 cm^{-1} (10% higher than water), surrounded the tumor to complete the filling of the cavity. The tumor was then located 7 cm from the posterior phantom edge and 10.5 cm from the lateral edge. An ^{131}I source of 29 μCi was placed anteriorly, initially in the midline of the phantom. Conjugate views (180° apart) of the "tumor" were acquired first without (15 min) and then with (5 min) the RC in place. These images were repeated over 9 days using a large field-of-view gamma camera with a high-energy collimator, interfaced with a computer. On Day 9, several RC positions different from the midline were tested.

Separate regions of interest (ROI) were drawn as rectangles around the tumor and RC. We investigated three methods of estimating background caused by tissue activity in front or behind the object of interest (Table 1). In the first method, it is assumed that background changes only gradually with position. The ROI of the RC in the tumor-only image is used to generate the background for both the tumor and RC. Correction is made for the size of the ROI and acquisition time when applying the background of the RC to the tumor. In the second method of background subtraction, the RC again obtains its background from the tumor-only image. The background of the tumor is estimated by drawing a larger rectangle around the tumor ROI and subtracting the activity of the tumor from this larger ROI. Correction is made for ROI size and acquisition time. In the third method, the background of the RC is determined by subtracting the activity of the RC from a larger rectangle which surrounds the RC. The background of the tumor is calculated similarly, as in Method 2.

TABLE 1
Methods of Background Subtraction

	RC background	Tumor background
1	From RC position in tumor only image	From RC position in tumor only image
2	From RC position in tumor only image	Area surrounding tumor ROI in tumor only image
3	Area surrounding RC in the RC + tumor image	Area surrounding tumor ROI in tumor only image

After background was subtracted by one of the three techniques, the geometric mean of the count rate for the tumor, C_T, and that of the RC, C_{RC}, was calculated from the anterior and posterior values (for anterior net counts A and posterior net counts P, the geometric mean is given by $[A \cdot P]^{1/2}$). Knowing the activity of the RC, A_{RC}, measured by a dose calibrator, the activity in the tumor A_T, was then found by the equation:

$$\frac{A_T}{A_{RC}} = \frac{C_T}{C_{RC}} \qquad \text{(Appendix I)}$$

For the anthropomorphic phantom, the ratio of the calculated tumor activity over the true tumor activity, T_T, was calculated:

$$R = \frac{A_T}{T_T}.$$

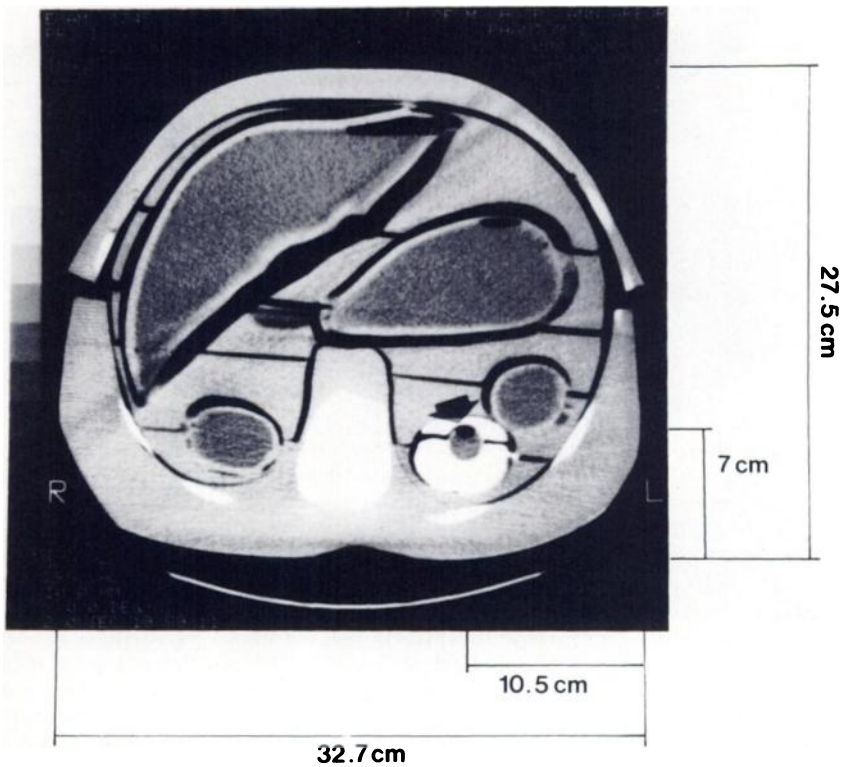

FIGURE 1
A computed tomographic image of the anthropomorphic phantom at the level of the kidneys. The "tumor" is indicated by the arrow. The dimensions (cm) of the phantom and distances of the "tumor" from the phantom edge are shown.

To test the effect of choice of ROI size, two different observers evaluated phantom data. Observer 1 consistently used an 8×8 pixel ROI for the tumor and RC and a 12×12 surrounding region, when necessary. Observer 2 consistently used regions 2 pixels larger in both directions.

Patients with pheochromocytoma enabled us to evaluate this method by examination of the decay of the RC, by checking the variation of apparent tumor uptake with RC position, and by comparing the calculated tumor uptake with the actual tumor content of radioactivity in 2 patients. Five patients with pheochromocytoma received 1.0 mCi/1.7 m^2 [^{131}I]MIBG intravenously. Views of the head, chest, abdomen and pelvis were obtained daily for 4 to 6 days using a large field-of-view gamma camera equipped with a high energy collimator interfaced with a computer. (Patients whose pheochromocytoma was excised were imaged for 2 days only). Reference sources of radioactivity (initially ~30 μCi, range 24–34, later 50–100 μCi) were placed on the anterior surface of the patient in an area near the tumor but separated from any distinct concentrations of [^{131}I]MIBG within the patient. Conjugate views were obtained, ROIs were drawn and background was determined as for the anthropomorphic phantom (Fig. 2).

In the case of the tumors from two patients, volume was both estimated from computed-tomography or magnetic-resonance imaging and also subsequently determined by weighing the excised tumors, assuming a density of 1 g/cm^3.

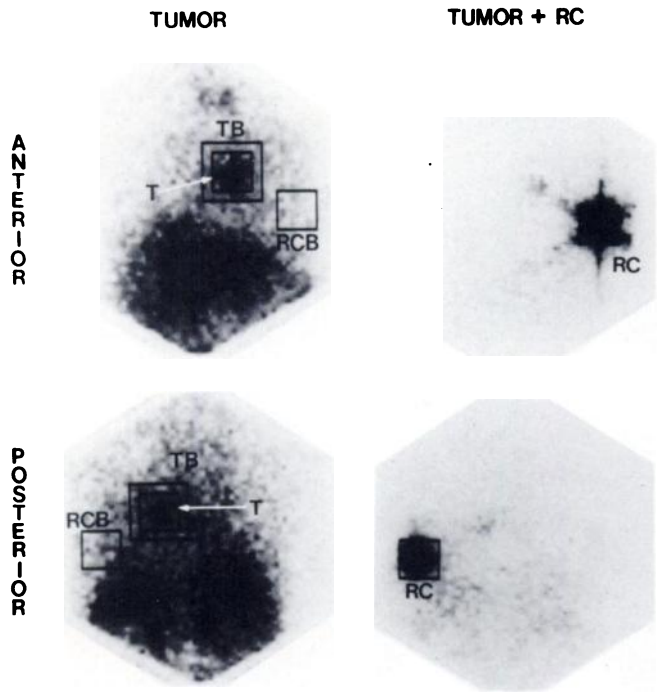

FIGURE 2
The image set required to determine uptake consists of anterior and posterior images of 15 min each (left) and the same pair for 5 min each with a known-activity reference source (RC) placed on the anterior skin (right). Shown is Patient 2 with a pheochromocytoma surrounding the pulmonary artery. (The RC, being more radioactive, overpowers the pheochromocytoma in the Reference + Tumor images.) The regions of interest are those needed for the second method of background subtraction with T being tumor, TB tumor background, RC reference source and RCB reference background.

RESULTS

Anthropomorphic Phantom

The "tumor" activity was measured for a midline RC position over 9 days using method 1 by observer 1 (Fig. 3). It decreased exponentially with a half-life of 8.25 days, in good agreement (+2.6%) with the half-life of ^{131}I of 8.04 days. This measurement shows that conjugate-view imaging can be used to track the time behavior of tumor uptake, at least if the background is not changing. The error in absolute activity averaged over the 9 days was 3.2%.

RC Position. On Day 9, 4 RC positions different from the midline position were tested. As seen in Figure 3, the "tumor" uptakes did not agree. Placement of the RC over the lung (a high transmission region), a distant choice for kidney tumor, gave an uptake 41% low: (measured-true)/true = −41%). Thus, one can infer that the 18% low activity (Fig. 3), calculated for one of the other nearby RC positions may have been partly caused by high transmission through the phantom at that position as well.

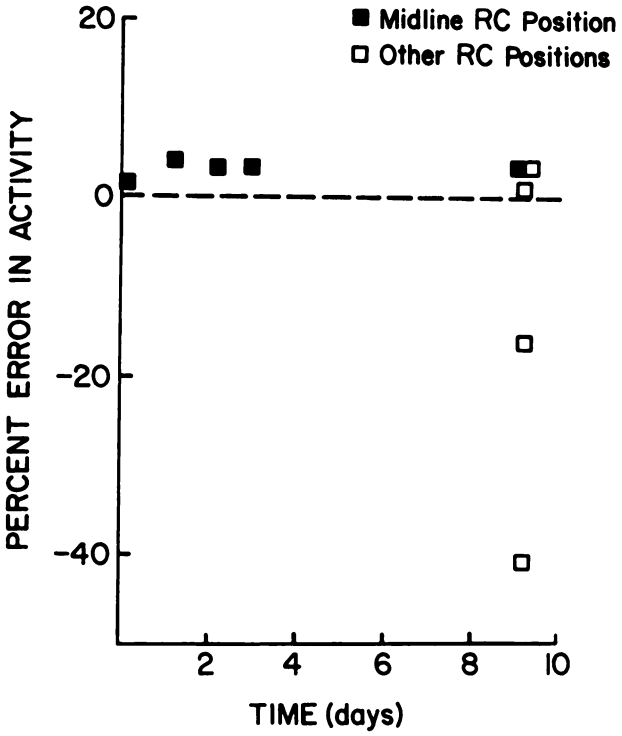

FIGURE 3
Percent error in activity calculated for a "tumor" in an anthropomorphic phantom by Method 1. For a midline RC position, the error is shown over 9 days. On Day 9, the error was shown as a function of RC position.

The effect of the different methods of background subtraction is shown in Table 2. It gives the values calculated for R on each day of imaging with the value on day 9 being the average over the four nearby RC positions. Method 1 gives the best values while Method 2 is about 14% low and Method 3 about 11% high.

To check on the significance of this trend, Figure 4 shows the magnitude of variation between observers for the same images. It is seen that the relative order of uptakes is the same between observers but that the absolute values for the second observer are lower by ~7%, making Method 3 the most accurate for him.

Lastly, for the two observers, the standard deviation of the mean for R with the 4 RC positions on Day 9 is tabulated in Table 3. There are similar findings between the two: Method 2 has the desirable feature of the least deviation and Method 3 the undesirable feature of the greatest.

The results from the phantom, then, are mixed: Methods 1 or 3 give the best absolute values, depending on observer, but Method 2 has the least dependence on choice of RC position.

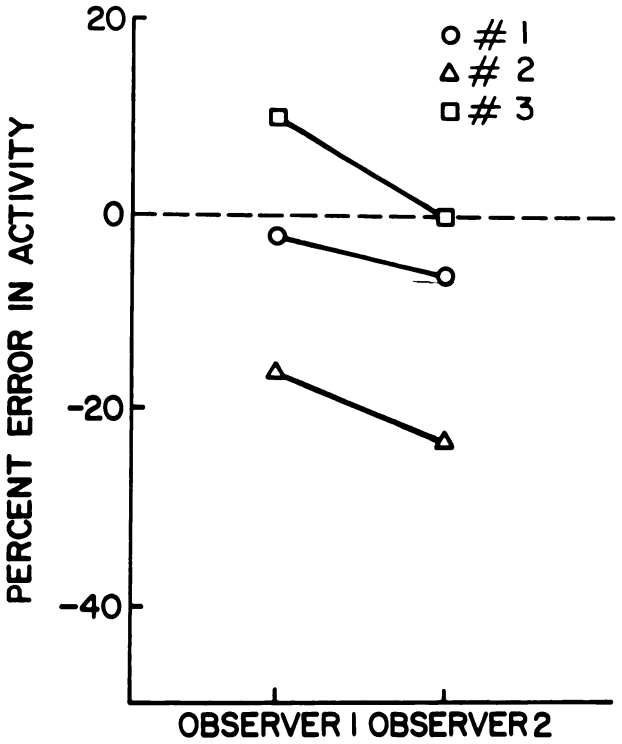

FIGURE 4
Percent error in activity averaged over four RC positions as calculated by two different observers. The parameter in the key is the background subtraction method. Judged by this test, the second method appears inferior in accuracy compared to the other two.

Patient Studies

Time Dependence. From a patient with pheochromocytoma, the activity of the ^{131}I RC is plotted in Figure 5. It is evident that the decay of the source, as determined from the geometric mean of the counts from the anterior and posterior images, approximates the decay of ^{131}I predicted by standard calculations. Therefore, RC activity determined by the camera method on a patient declines in a predictably reliable, exponential form.

Variation of tumor uptake with RC position. Figure 6 shows the variation in estimated tumor uptake with RC position for Patient 3. Since the true value isn't known, the absolute difference from the average on a given day is calculated. It is seen that the variation with method 1 is much larger than with either Method 2 or 3. The results are similar with the other patient except that with Method 1, the computed uptake actually becomes a negative and impossible value in some cases.

TABLE 2
Ratio of Calculated Value Over True Value, R, for Anthropomorphic Phantom and Observer 1

	Day				
Method	0	1	2	3	9*
1	1.02	1.04	1.03	1.03	0.978
2	0.866	0.871	0.865	0.869	0.841
3	1.11	1.10	1.14	1.08	1.10

* Values for this day are average values over four different RC positions.

Surgically excised pheochromocytomas. Patient 1 is a 25-yr-old man with multiple endocrine neoplasia. Patient 2 is an 18-yr-old man who underwent extirpation of a pheochromocytoma surrounding the pulmonary artery.

Table 4 shows the calculated activity with that measured in vitro for the two patients. There is a fair range of calculated values depending on the background subtraction used. For Patient 1, the third method gives the result closest to that measured by tissue counting. For Patient 2, the activity is much lower and the second and third methods give values within the range of the tissue measurement.

In patients who exhibit background activity, the results for different background methods differ from those found for the phantom, which had no background activity. Also, they are no longer mixed depending on

TABLE 3
Standard Deviation in R Over Four RC Postions Anthropomorphic Phantom on Day 9

Method	Observer 1	Observer 2
1	0.18	0.18
2	0.15	0.13
3	0.29	0.21

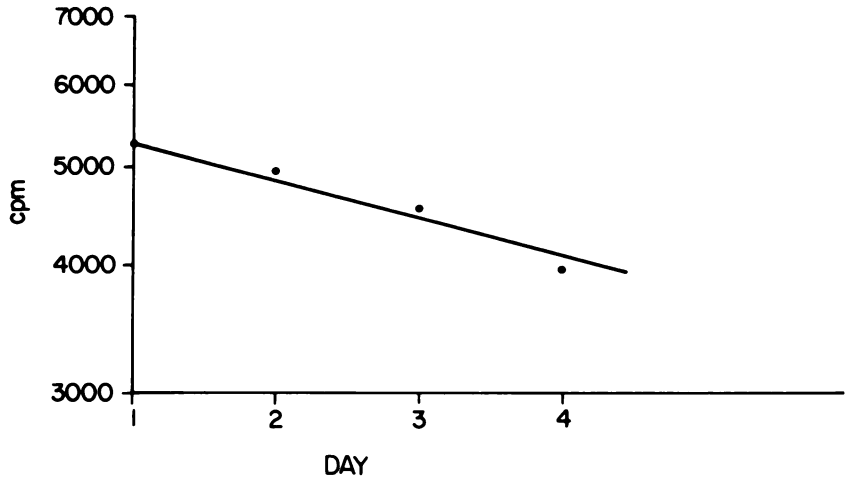

FIGURE 5
Semilog plot of calculated counts per minute versus time in days. The straight line is from the known decay constant of ^{131}I. The data points are from image data for the RC in place on the skin of the patient.

the criterion for judging quality. In the patients, either Method 2 or 3 gives both good absolute values and also the desirable feature of small variation with RC position.

DISCUSSION

There are multiple variables that a method of predicting radioactivity content in an internal structure faces. Sensitivity of the detector may vary day to day. Attenuation of gamma-rays by overlying tissues reduces the photon flux reaching the camera. Septal penetration varies with distance and can impair resolution and the precise definition of tumor borders. Compton scatter within the patient changes the photon flux which is included within the photopeak window. Differences in selection of region of interest can cause variations in calculations of net tumor uptake. A reasonable estimate of tumor volume is likewise necessary to accurately predict density of tumor radioactivity content, and thus delivery of radiation absorbed dose.

The conjugate view method, using a reference source with known activity, compensates for many of those variables. Errors produced by changes in efficiency of the detector are cancelled by parallel effects on the RC and tumor. The use of the geometric mean should correct for variation of attenuation with depth of the tumor within the body. Our method appears somewhat simpler than that of Thomas (*3,4*) in that it requires no separate calculation of attenuation. The third background subtraction method specifically tries to account for septal penetration by ignoring an otherwise good background estimate for the RC in order to choose one that has a similar degree of septal penetration as for the tumor.

Location of the RC greatly influences the estimates of tumor uptake-RCs in the midline and close to the tumor appearing most reliable. We had originally considered placement of the RC directly over the tumor but this proved difficult and subject to greater day to day variability, since external landmarks were often not precisely anterior to the tumor. Likewise, when the RC lies directly over the tumor, the determination of counts from RC activity in the posterior images, and thus the net counts attributed to the RC tumor, becomes less reliable as tumor uptake approaches the activity of the RC.

RC activity is also important in the determination of appropriate RC borders. In our initial experience, mocks of ~30 μCi of ^{131}I or less occasionally provided imprecise RC borders and low count rates for the posterior view. Raising the RC radioactivity to 50–100 μCi has obviated these difficulties and allows ready visualization of the RC on the posterior as well as the anterior view. With a 100 μCi ^{131}I source, assuming an exposure of 15 min daily for 5 days and an average skin distance of 1 cm, the additional radiation dose to the skin is only 3 rad, of small consequence when compared to the internal administration of up to 200 mCi of [^{131}I] MIBG for therapy.

Since it is a total procedure, trying to answer the question "Which of the factors being accounted for is causing the most error in calculated activity?" is difficult. However, the largest single source of error in calculating clinical tumor dosimetry is probably estimation of tumor size (*5,6*) in any case. The tissue measurements show how complicated this problem is. There was considerable variability in uptake within one tumor ranging nearly twofold. In addition, areas of hemorrhage and necrosis may contribute to tumor volume as seen on computed tomography or magnetic resonance imaging without accumulating radioactivity and being involved in the first-order dosimetry calculation. Narrowing the distance between imaging planes and refinements in distinguishing tumor borders should reduce the error contributed by volume estimation.

We believe this method of conjugate views provides a reasonable basis from which tumor uptake, and thereby, dosimetry can be approached. Use of a reference source allows for the cancellation of errors that

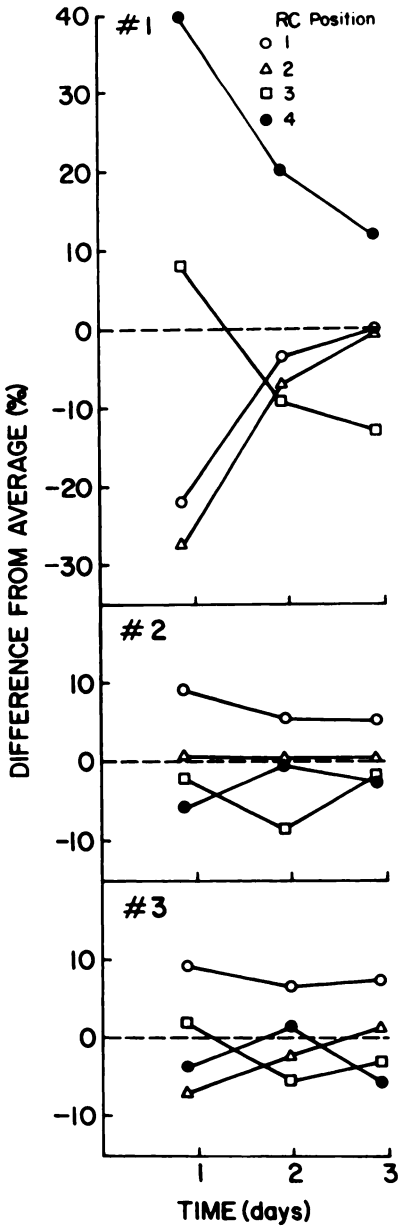

FIGURE 6
The calculated activity with a given RC position is subtracted from the average value for all positions. The differences are found for 3 imaging days and with the method as a parameter. For this patient, Method 1 has an undesirably large variation with RC position.

affect radioactivity determinations, including those from instrument variability, soft tissue attenuation and septal penetration. As the accuracy of single photon emission computed tomography is improved, it may be utilized to acquire a complete set of uptake-versus-time results, further improving the precision of dosimetric estimation. At present, we maintain that this method provides clinically valuable estimates of ^{131}I activity in tumors which can be the basis for planning radiopharmaceutical therapy and analyzing the effects of such therapy.

TABLE 4
For Excised Tumors, A Comparison of Radioactivity Concentration Calculated by Different Background Subtraction Methods And That Measured by Tissue Counting

	Calculated concentration* of ^{131}I (nCi/g)			
	Background subtraction method			Measured concentration
Patient	1	2	3	of ^{131}I (nCi/g)
1	880	560	700	750
2	47	31	37	20–40

* Calculated concentration = calculated activity/calculated volume.

APPENDIX 1

$A_T = \frac{(I_A\ I_P)^{1/2}}{(e^{-\mu ct})} \frac{f}{E}$ for a single tumor in zero background (3).

If the tumor is a point, then f = 1.
Assuming the transmission can be measured with an uncollimated source, then

$$RC_P = e^{-\mu ct} RC_A$$

where

RC_P = posterior reference source counts.
RC_A = anterior reference source counts.

Also assuming the camera efficiency constant, E, can be measured with the patient behind the source, then

$$E = RC_A/A_{RC} = \text{reference source activity}$$

substituting

$$A_T = \frac{(I_A\ I_P)^{1/2}\ (RC_A)^{1/2}}{(RC_P)^{1/2}} \times \frac{A_{RC}}{RC_A} = \frac{(I_A\ I_P)^{1/2}}{(RC_A \times RC_P)^{1/2}} \times A_{RC}$$

then

$$\frac{A_T}{A_{RC}} = \frac{(I_A\ I_P)^{1/2}}{(RC_P)^{1/2}} = \frac{C_T}{C_{RC}},$$

where

C_T = geometric mean of the tumor counts
C_{RC} = geometric mean of the reference source counts.

ACKNOWLEDGMENTS

This work was supported by PHS Grant #DK21477 awarded by the National Institute of Diabetes and Digestive and Kidney Diseases, DHHS, and by PHS Grant #CA38790 awarded by the National Cancer Institute, DHHS. The authors give special thanks to Katie Workman for secretarial expertise.

REFERENCES

1. Sorenson JA. Methods for quantitating radioactivity in vivo by external counting measurements [Ph.D.

thesis]. University of Wisconsin, 1971.
2. Sorenson JA. Quantitative measurement of radioactivity in vivo by whole-body counting. In: Hine GJ, Sorenson JA, eds. *Instrumentation in nuclear medicine*. Vol. 2. New York: Academic Press, 1974:311–348.
3. Thomas SR, Maxon HR, Kereiakes JG. In vivo quantitation of lesion radioactivity using external counting methods. *Med Phys* 1976; 3:253–255.
4. Thomas SR, Maxon HR, Kereiakes JG, Saenger EL. Quantitative external counting techniques enabling improved diagnostic and therapeutic decisions in patients with well-differentiated thyroid cancer. *Radiology* 1977; 122:731–737.
5. Maxon HR, Thomas SR, Hertzberg VA, et al. Relation between effective radiation dose and outcome of radioiodine therapy for thyroid cancer. *N Engl J Med* 1983; 309:937–941.
6. Adler RS, Koral KF, Carey JE, Kline RC, Beierwaltes WH. Two-orthogonal-view method for quantification of rad dose to neck lesions in thyroid cancer therapy patients. *Med Phys* 1982; 9:497–505.